Modification of bedrock surfaces by glacial abrasion and quarrying: evidence from North Wales

N.F. Glasser[1], M. Roman[2], T.O. Holt[1], M. Žebre[1], H. Patton[3], A.L. Hubbard[1,3]

[1]Department of Geography and Earth Sciences, Aberystwyth University, Ceredigion, Wales SY23 3DB.

[2]Department of Geography, Faculty of Science, Masaryk University, Kotlářská 2, 611 37 Brno, Czechia

[3]CAGE - Centre for Arctic Gas Hydrate, Environment and Climate, Department of Geosciences, UiT The Arctic University of Norway, 9037 Tromsø, Norway

Correspondence to Neil Glasser: nfg@aber.ac.uk

Abstract

Abrasion and quarrying are significant processes of subglacial erosion for ice masses in direct contact with hard substrates, yet their relative efficacy and spatio-temporal variability is unclear. Here, we investigate the glacial impact of these processes on a 70 m by 60 m bedrock surface at Moel Ysgyfarnogod in the Rhinog Mountains, Wales, using a combination of high-resolution digital photographs, analysis of a Digital Terrain Model derived from an Unmanned Aerial Vehicle survey, and regional ice sheet modelling. We map and analyze the distribution of grooved and striated surfaces, abraded surfaces, quarried blocks and open fractures in addition to the orientation of pre-existing bedrock fractures and joints. The grooves and

striations are orientated in a single, consistent direction across the bedrock surfaces related to regional ice flow during the Late Pleistocene. Abraded and smoothed bedrock dominates the proximal edges of the bedrock outcrop and quarrying prevails on the distal edges of the bedrock outcrop, which are dominated by detached and partially detached blocks. We propose these blocks were removed during the final stages of the last glacial cycle when subglacial meltwater was plentiful in this otherwise predominantly frozen subglacial setting. A minimum estimate of 2000 m^3 displaced material at this site implies that subglacial quarrying would have been an important erosional process during final stages of deglaciation.

Key Words

Glacial erosion, subglacial bedrock surfaces, abrasion, quarrying

Introduction

Throughout the multiple ice age cycles that characterise the last ~2.6 Ma, subglacial erosion has had a profound influence on temperate and polar landscapes of both hemispheres (Sugden and John, 1976; Cook et al., 2020). Two of the single most important processes of glacial erosion beneath warm-based glaciers and ice sheets resting on hard beds are abrasion and quarrying. Abrasion describes the wear of a rock surface by rock debris in transport in basal ice (Hallet, 1979, 1996; Cohen et al., 2005) and produces elongated, streamlined landforms with smoothed and ice-abraded surfaces (Evans, 1996; Roberts and Long, 2005). Quarrying describes the processes involved in the detachment and removal of blocks of bedrock (Glasser and Bennett, 2004). It has been suggested that abrasion may dominate over other erosional processes beneath fast-flowing glaciers (Herman et al., 2015; Yanites and Ehlers, 2016), however, quarrying is arguably the more important of the two processes because it provides the basal material required for glacial abrasion (Alley et al., 2019).

Quarrying theory defines the basal conditions that favour the growth of cracks in otherwise coherent bedrock (Iverson, 1991; Hallet, 1996). In addition to the role of basal sliding, which supplies the frictional energy, the important relationships are those of effective pressure of ice on the bed (ice overburden load minus subglacial water pressure) and the primary role of ice-bed cavities, usually in the lee of a rock step. The presence of cavities has the effect of concentrating stresses on rock protuberances. Under certain conditions, high effective ice pressures can hydraulically fracture and open existing or new micro-cracks normal to ice flow, and allow the removal of blocks of rock. Rapidly fluctuating water pressures in such cracks enhances fracture propagation and quarrying, which has been demonstrated by several empirical and theoretical studies (Iverson, 1991; Hallet, 1996; Cohen et al., 2005; Bartholomew et al. 2011; Anderson, 2014; Ugelvig et al., 2018). Diurnal and seasonal melt variations, and thus subglacial water pressure, can have an even more pronounced effect on the rates of quarrying since of the temporal amplification of differential bedrock stress around cavities and promotion of crack growth (Ugelvig et al., 2018). The imbalance between cavity size and water pressure drives episodes of elevated stress on the upglacier edges of steps in the bed, the so-called “hammer effect” by Anderson (2014), which is potentially of importance also for the quarrying rates integrated over longer periods (Ugelvig et al., 2018). According to Anderson (2014) thicker ice will generate a greater frequency of hammer events and thus is more effective at quarrying than thinner ice due to increased short-term oscillations in the sliding system. Stick-slip motion may also play a role in subglacial erosion (Zoet et al., 2013).

There are well-established links between lithology, bedrock structure and the geometry of glacial erosional landforms (Glasser et al., 1998). The importance of pre-existing fractures for quarrying processes is confirmed by field observations (Jahns, 1943; Gordon, 1981; Krabbendam and Glasser, 2011; Lane et al., 2015, Krabbendam et al., 2017), and the relationship between pre-existing fractures and quarrying has also been modelled theoretically (Iverson, 2012, Hooyer et al., 2012, Anderson, 2014). Geological data (e.g. measurements of concentrations of cosmogenic ^{10}Be in glacial polish and bedrock fracture spacing) suggest that the distance between fractures in the rock are particularly important (Dühnforth et al., 2010). Quarried surfaces and major joint sets are often coincident (Hooyer et al., 2012). This is because the relative importance of abrasion and quarrying as geomorphic agents, and therefore bed roughness, is controlled by fracture spacing (Iverson, 2012; Anderson, 2014). Hardness and joint spacing also exert a strong control on subglacial erosional landforms and the mechanisms that form them (Krabbendam and Glasser, 2011).

Sugden et al. (1992) suggested that quarrying is also enhanced at the edge of a receding or thinning ice sheet, partly because of the changing relationship here between ice velocity and effective pressure. They argued that ice is thinner close to the margin and the normal load is lower, so cavities are likely to be more abundant and there is higher meltwater production. Assuming the ice is actively flowing, it becomes easier for overriding ice to dislodge and evacuate blocks close to an ice margin. These blocks often travel only short distances (metres) and their provenance can be traced to proximate source locations, further supporting the notion that an intense episode of quarrying accompanies deglaciation (Sugden et al., 2019). In numerical experiments, Ugelvig et al. (2018) also considered that meltwater variability enhances quarrying the most where there is a flat bed and thick ice, while abrasion is more sensitive to the variations in their steeper bed, thinner ice experiment. They observed that quarrying is most sensitive to variations in effective pressure, which are greatest in the thick-ice experiments, while larger variations in sliding speed boosts abrasion the most in the experiment with the steeper bed. Alley et al. (2019) noted that rapid, sustained bedrock erosion requires till removal at the ice/bed interface by sediment transport in subglacial streams.

Studies of subglacial erosive processes generally focus on temperate/wet basal conditions because these promote sliding. It is generally held that cold or polythermal ice masses characterized by frozen bed conditions preclude such processes and act to protect their substrates and indeed, may even shield inherited pre-glacial landscapes. In recent decades, this view has been challenged both from process-glaciological and glacial geomorphological perspectives (e.g., Cuffey et al., 2000; Atkins et al., 2002; Atkins, 2013). Direct observation of active subglacial sediment entrainment under thermal conditions of −17 °C recorded in the basal layers of Meserve Glacier in the Dry Valleys, Antarctica, demonstrates that the assumption that cold-based glaciers do not slide and abrade their beds is incorrect (Cuffey et al., 2000). Although rates of subglacial abrasion may be an order of magnitude lower than those observed at warm-based ice masses, these observations suggest that even under prolonged cold-based conditions, given sufficient basal traction, basal sliding and associated erosion will occur. These findings are supported by geomorphological observations from formerly glaciated landscapes in the same region of Antarctica; for example, Atkins (2013) mapped the glacial geomorphological features across the forefield of frozen-based glaciers in the Dry Valleys, Antarctica.

Here, we address these questions about the styles and relative efficiency of glacial erosion with reference to a palaeo-glaciated bedrock surface at Moel Ysgyfarnogod in the Rhinog Mountains, Wales. We combine detailed analysis of DTM and fine-resolution imagery acquired by Unmanned Aerial Vehicle (UAV) with regional ice flow modelling to investigate the distribution and relative efficacy of abrasion and quarrying processes along with their former subglacial thermal regime across a 60 x 70 m area of the bedrock pavement. Our mapping and analysis of the distribution of geological, geomorphological and glacial characteristics of the Moel Ysgyfarnogod bedrock pavement enables us to qualitatively assess the relative efficacy and spatio-temporal distribution of the subglacial erosional processes operating beneath the ice mass that occupied the Rhinogs during the late Pleistocene. Similar glacial geomorphological mapping studies of bedrock pavements elsewhere in Wales, such as Snowdon (e.g. Sharp et al., 1989), provide additional context for our findings here.

Study Area

The Rhinog Mountains (*Rhinogydd* in Welsh) are located in North Wales (Figure 1). Geologically they are part of the Harlech Dome, a large anticline composed of Cambrian sandstones and mudstones of the Rhinog Formation and sandstones of the Hafotty Formation (EDINA Geology Digimap, 2014). The latter rock type forms the summit areas of most of the northern Rhinog Mountains, including the highest local summit at Moel Ysgyfarnogod (623 m asl), close to our chosen study site. The Rhinog Mountains were formerly covered by the Welsh Ice Cap, one of the constituent components of the former British-Irish Ice Sheet (BIIS). The Welsh Ice Cap was largely independent of the BIIS, which had its thickest centres over Ireland, England and Scotland. The evidence of the pre-Devensian (pre-LGM) glaciations in Snowdonia has been mostly obliterated by the erosive action of the last Welsh Ice Cap at the LGM (Sharp et al. 1989). However, there are several localities in Britain, such as the Sudbury Formation in the Kesgrave proto-Thames Terrace sequence, with far-travelled erratic material from north Wales, that indicate presence of mountain glaciers and ice caps in the Middle and possibly Early Pleistocene, namely during the Anglian and Wolstonian stages (Lee et al., 2011). Data on the recession of the Welsh Ice Cap are scarce but Glasser et al. (2012) provided eight paired $^{26}Al/^{10}Be$ exposure ages from the Aran mountain summits and established that these summits were exposed at c. 20–17 ka. Thinning of the Welsh Ice Cap after this time was rapid (Hughes et al., 2016).

The Rhinog Mountains are situated close to the centre of the Welsh Ice Cap at the Last Glacial Maximum (LGM), lying just to the west of the main ice divide (Fearnsides 1905; Greenly 1919; Ball and Goodier, 1968; Foster 1968, 1970a,b; Addison 1997; Jansson and Glasser 2005; Glasser et al., 2012; Patton et al. 2013a, b). All areas of the mountains above ~550 m asl are dominated by large, gently dipping glacial bedrock pavements with scattered angular and subangular glacially transported boulders (Figure 2). The surface of the bedrock is striated and grooved. On the lower elevation slopes below our study area are glacial meltwater channels. The age of deglaciation is constrained by three cosmogenic isotope exposure ages collected from a bedrock surface and boulder at nearby Moel Ysgyfarnogod at a similar elevation to our study site (Hughes et al., 2016). These are a striated bedrock sample (19.39 ± 0.97 ka) and a paired striated bedrock / boulder sample (20.26 ± 0.96 ka and 17.86 ± 0.81 ka respectively).

Our plot is located on a flat, near-horizontal striated bedrock surface around 550 m asl (52°53′14″ N, 3°59′46″ W). The modelled former ice-surface elevation at the LGM was around 1000 m asl (Patton et al. 2013a) suggesting the study site lay beneath at least 400 m of ice at the LGM. Our specific study area is a ~70 m by 60 m glacially abraded and quarried rock pavement bounded by 3-5 m high cliffs on all sides (either dropping down or forming a wall above leading to another level of rock pavement).

Methods

Digital photographs of the bedrock surface were collected using an Unmanned Aerial Vehicle (UAV; DJI Phantom 4) equipped with a DJI FC300C camera (12 MP resolution) and GPS from c. 4–6 m above the ground surface. 'Structure-from-Motion' processing was undertaken in AgiSoft Professional software using standard and documented procedures for applied photogrammetric analysis in glacier and geomorphic studies (e.g., Westoby et al., 2012; Ryan et al., 2015; Jones et al., 2018). In total, 872 photographs were aligned and a dense point cloud was created, containing 254,786,611 points. The dense point cloud was then used to create a high-resolution orthophotograph (pixel size $2.33\cdot10^{-3}$ m) and Digital Terrain Model (DTM, $4.67\cdot10^{-3}$ m per pixel) from which a slope map was calculated in ArcMap 10.7.3. Geospatial coordinates were taken from the onboard GPS without the need for ground control points. Overlaying our orthophotograph onto georeferenced aerial imagery showed good agreement between the two datasets, with vertical and horizontal offsets no greater than 2 m, and an orientation offset of no more than 2°. In ArcMap we used the orthophotograph and DTM to characterize styles of glacial erosion by manually digitising all major features of glacial erosion on the exposed bedrock surfaces, including glacial grooves and striations, quarried blocks, glacially transported and perched boulders, and bedrock structures such as fractures and joints. Blocks which have clearly toppled or fallen from cliff edges post-glacially around the edges of the plot were not mapped. These toppled blocks are easy to identify because their abraded surfaces are no longer upward-facing. The orientation of grooves, striations, bedrock fractures and joints were calculated using Zonal Geometry as Table statistics in ArcMap. Determination of blocks displacement and topographic profiles was performed in QGIS 3.8.1.

Geomorphology Results

Based on our DTM analysis, we identify the following five primary components of the glacially-eroded landscape (Figure 3).

Striations and grooves

Striations and grooves occur on the upper surfaces of the bedrock across the entire study area, with grooves continuous for distances of up to 4 m (but more typically 2 m, with a mean length of around 0.5 m). Most striations are only a few mm in width and depth, as deduced from the orthophotograph, though grooves several cm wide (and deep) can be discerned from DTM and are particularly well highlighted using slope shading. Overall, 1674 striations were delimited, with a strong east-west preferred orientation (85 - 265 to 110 - 290°) (Figure 4A).

Abraded bedrock surfaces

The eastern proximal flank of the bedrock pavement is smoothed, and the cliff edges are rounded and ice-moulded (Figure 5). The cliff edges are intact, although there are a few partially quarried and detached blocks along the cliff edge.

Quarried bedrock

The cliff edge on the western distal flank of the bedrock pavement is characterised by quarried blocks and open bedrock joints (Figure 6). Quarried blocks are angular and in places joints and fractures of up to 0.74 m wide and up to 4 m deep are open between individual blocks. The furthest travelled block that we could identify with a high level of confidence by matching to the original cliff face was 1.45 m, and this particular block (near the south cliff edge; Figure 3) was rotated a few degrees from its original orientation as evidenced by striations. Open joints and fractures are visible at distances as far as 25 m inwards of the quarried cliff edge. Vegetation obscures a number of open bedrock joints and fractures where they are filled or partially filled with regolith and soil; these were therefore not delimited. Based on the mapping, the largest reliably quarried blocks have a volume of at least 180 m^3 (based on an area of 45 m^2 multiplied by depth of 4 m). This is a conservative estimate, and represents a minimum value because it is based on a maximum fracture depth of 4 m; some fractures were deeper than this but could not be measured beyond 4 m in the field. The volume of quarried or partially quarried bedrock blocks at Moel Ysgyfarnogod at the time of deglaciation is therefore at least 2000 m^3 (based on the area of rock pavement with open joints, measuring 50 x 10 m with a depth of at least 4 m).

Glacially transported boulders

The surface of the rock pavement is littered with perched cobbles and boulders of presumed glacial origin (Figure 3). Although they are similar lithology to the bedrock pavement itself, the boulders are typically subrounded or subangular and display evidence of subglacial abrasion. There are also occasional angular boulders, which appear to have been moved only short distances. It is possible that these angular boulders have moved only within the local vicinity after being plucked upwards from the bedrock pavement nearby.

Bedrock joints and fractures

Mapped bedrock joints and fractures show an overall NE-SW orientation. Detailed measurements reveal a slightly more complicated picture of a multimodal distribution with three consistent orientations 25–205°, 40–220°and 60–240° (Figure 4B). The orientation of bedrock joints and fractures contrasts with the orientation of the mapped striations and grooves, which have a strong preferred east-west orientation (Figure 4A).

Interpretation and Discussion

Well-developed striations and grooves are present across the entire surface of the bedrock outcrop, but quarried surfaces are restricted to the down-ice (lee) side of the bedrock at Moel Ysgyfarnogod. The distribution of abraded and quarried surfaces therefore fits existing glacial erosion theory, which predicts that ice-moulded and abraded surfaces should dominate the up-ice (stoss) side of bedrock outcrops and quarrying should dominate the down-ice (lee) side of bedrock outcrops. The overall distribution of the abraded and quarried surfaces is therefore consistent with an inferred ice movement direction across the study area from approximately east to west, and reflects relatively stable and long-term ice maximum conditions of the LGM (Foster, 1970a; Sharp et al. 1989).

There is a strong relationship between quarrying of blocks and bedrock structure at Moel Ysgyfarnogod. Quarrying, and the subsequent movement of large blocks, is strongly linked to the structure of the bedrock, especially the joints and fractures, which collectively define lines of weakness; open joints are visible in the bedrock at distances of up to 25 m from the quarried cliff edge. Blocks were thus moved mainly to the southwest, despite the general ice flow direction from east to west. The consistent west to east alignment of the striations and grooves (median azimuth = 99–279°) indicates ice flow was orthogonal to the bedrock fractures and joints (median azimuth = 37–217°), which may have enhanced bedrock quarrying (Jahns, 1943; Gordon, 1981; Krabbendam and Glasser, 2011; Hooyer et al., 2012; Iverson, 2012; Anderson, 2014; Lane et al., 2015; Krabbendam et al., 2017).

Based on a best-match of the edges of quarried blocks to their source-location in the adjoining cliff (akin to fitting jigsaw-pieces), we determined the displacement vector (distance and direction) of the centroid of each of the blocks (Figure 6). The predominant displacement vector was to the southwest (mean = 225°), i.e., slightly offset from the overall direction of ice flow but aligned with the orientation of bedrock joints and fractures. However, on the proximal side of the cliff, the travel direction is mostly eastward, and follows the general slope gradient. Postglacial, paraglacial or gravitational influences cannot be completely excluded, though this is only likely to apply to smaller blocks. Large blocks on the west side around the Area 2 will be less affected by postglacial, paraglacial or gravitational influences since the overall bedrock surface is approximately level (Figure 5). The mean distance of displaced blocks that can be matched with confidence to the source cliff is 0.29 m. There is also a clear relationship between bedrock joint and fracture orientations and the displacement of the quarried blocks, visible in Figs 4 and 6 (Dühnforth et al., 2010; Hooyer et al., 2012).

The analysis can be used to illuminate the relative efficacy of quarrying versus abrasion at the study site. It has been argued that abrasion dominates other subglacial erosional processes beneath fast-flowing glaciers (Herman et al., 2015; Yanites and Ehlers, 2016). At Moel Ysgyfarnogod, however, it is apparent that quarrying was the most important process. We have identified a number of large blocks that appear to have been in the process of being rotated away or dislodged from the bedrock outcrop. Given the freshness of these quarried surfaces we assume that quarrying took place during deglaciation, coeval with ice thinning and retreat, although it is of course possible that the quarried surface pre-date deglaciation. The timing of the glacial erosion is discussed below. The volume of bedrock quarried at Moel Ysgyfarnogod at the time of deglaciation is high; at this bedrock pavement alone, the volume of quarried or partially quarried bedrock blocks bounded by open joints is equivalent to at least 2000 m^3. Given an approximate bulk density of sandstone of 2300 kg m^3, we estimate that ~4600 tonnes of rock was subglacially quarried and subsequently displaced by the overriding ice during deglaciation.

We infer that subglacial bedrock quarrying was active during a phase characterised by warm basal conditions with an abundant supply of meltwater. We speculate that this transition from cold to temperate/warm basal conditions was coincident with final phases of deglaciation, as the Welsh Ice Cap thinned and retreated locally due to enhanced atmospheric temperatures. Such a scenario is consistent with studies demonstrating rapid thinning of the ice cap after c. 20 ka (Hughes et al., 2016). Enhanced quarrying during deglaciation beneath thinning ice is also likely because this favours the formation of subglacial cavities as well as rapid and high magnitude short-term fluctuations in subglacial water pressure under enhanced temperatures and associated rainfall events (e.g., Doyle et al., 2015).

This interpretation is further supported by numerical modelling of the Welsh Ice Cap which demonstrates that even though persistent thick ice cover was present at the site, it was at the pressure melting point for a short period of ~1000 years coincident with final deglaciation (Patton et al., 2013a, b) (Figure 7). Given that the bedrock pavement demonstrates extensive glacial erosion under predominantly warm-based conditions, it follows that intense glacial erosion must have been active over a short time-span. If so, this implies that a late phase of quarrying accompanied deglaciation as the Welsh Ice Cap thinned locally over this area. Nearby cosmogenic exposure ages constrain deglaciation to a minimum age of 20 ka (Hughes et al., 2016).

Regional modelling of the outlet glacier dynamics of the Welsh Ice Cap that drain into Cardigan Bay and Irish Sea support this proposition (Patton et al., 2013c). Early debuttressing of the western ice margin after retreat of the Irish Sea ice stream gave westward-draining outlet glaciers of the Welsh Ice Cap the space to temporarily readvance into Cardigan Bay during episodes of climatic warming with increasingly maritime conditions associated with Heinrich Stadial 1 (Figure 8). We speculate that the quarrying and transportation of blocks at Moel Ysgyfarnogod likely occurred during these short but intense phases of glacial readvance, fast-flow and interior draw-down when favourable ice conditions (thin ice, abundant meltwater, subglacial cavity formation, rapid sliding) dominated. The modelled flow regime demonstrates that glacial motion across the Rhinogs during the latter stages of glaciation (Heinrich 1) was orientated from the northeast to southwest, and became increasingly topographically constrained as regional ice was drawn-down and thinned. These results are consistent with the direction of palaeo ice flow determined from block displacement at our field-site at Moel Ysgyfarnogod.

This scenario suggests that the subglacial abrasion processes that gave rise to the ice-moulded features observed at Moel Ysgyfarnogod are likely to have preceded the episode of intense quarrying during final stages of deglaciation. Detailed examination of the glaciated pavement provides support for this scenario because we find evidence of ice-moulded and rounded blocks that are detached and displaced yet in which striations and general morphology match their adjacent upstream bedrock. Our analysis tantalizingly lends support for the proposition that at least some fraction of the observed abrasion could have been sustained under frozen subglacial conditions prevalent at the site throughout the majority of the last glacial (Cuffey et al., 2000; Atkins et al., 2002; Atkins, 2013). However, without further cosmogenic exposure analysis of these erosion surfaces (e.g., Glasser et al., 2012), such a proposition cannot be verified.

Finally, we note the value of our UAV data for palaeo-glaciological studies of this kind. UAV survey enabled the creation a sub-centimetre resolution DTM, while covering a relatively large study site. This demonstrates the potential for UAV and SfM techniques for glacial-geomorphological studies at the intersection between sub-millimetre-scale investigations of individual smaller outcrops such as weathering (Verma and Bourke, 2019), and larger-scale monitoring of glaciers and (peri-)glacial environments (Ryan et al., 2015; Piermattei et al., 2016; Groos et al., 2019).

Conclusions

1. The distribution of abraded and quarried surfaces at Moel Ysgyfarnogod confirms existing glacial erosion theory with ice-moulded and abraded surfaces dominating the up-ice proximal side of the bedrock outcrop and quarrying dominating the down-ice distal side of the bedrock outcrop.
2. Glacial quarrying shows a strong relationship with bedrock structure; large blocks are detached and partially detached along pre-existing fracture and joint sets.
3. There is evidence that glacial quarrying can rapidly remove large amounts of bedrock; we estimated the volume of bedrock that was in the process of being quarried at the time of deglaciation at this one site alone to be equivalent to at least 2000 m^3.
4. We propose that quarrying dominated during a phase of warm-basal conditions with plentiful meltwater supply, presumably during final phases of deglaciation as the local ice cap thinned and the subglacial conditions required for quarrying (thin ice, rapid sliding, abundant meltwater, cavity formation) were fulfilled.

Acknowledgements

MR’s contribution was supported by the Masaryk University project MUNI/A/1356/2019 and Ministry of Education, Youth and Sports of the Czech Republic projects LM2015078 and CZ.02.1.01/0.0/0.0/16_013/0001708. AH and HP acknowledge support by the Research Council of Norway through its Centre of Excellence funding scheme (grant 223259) and HP the Akademia Programme at Equinor.

Figures

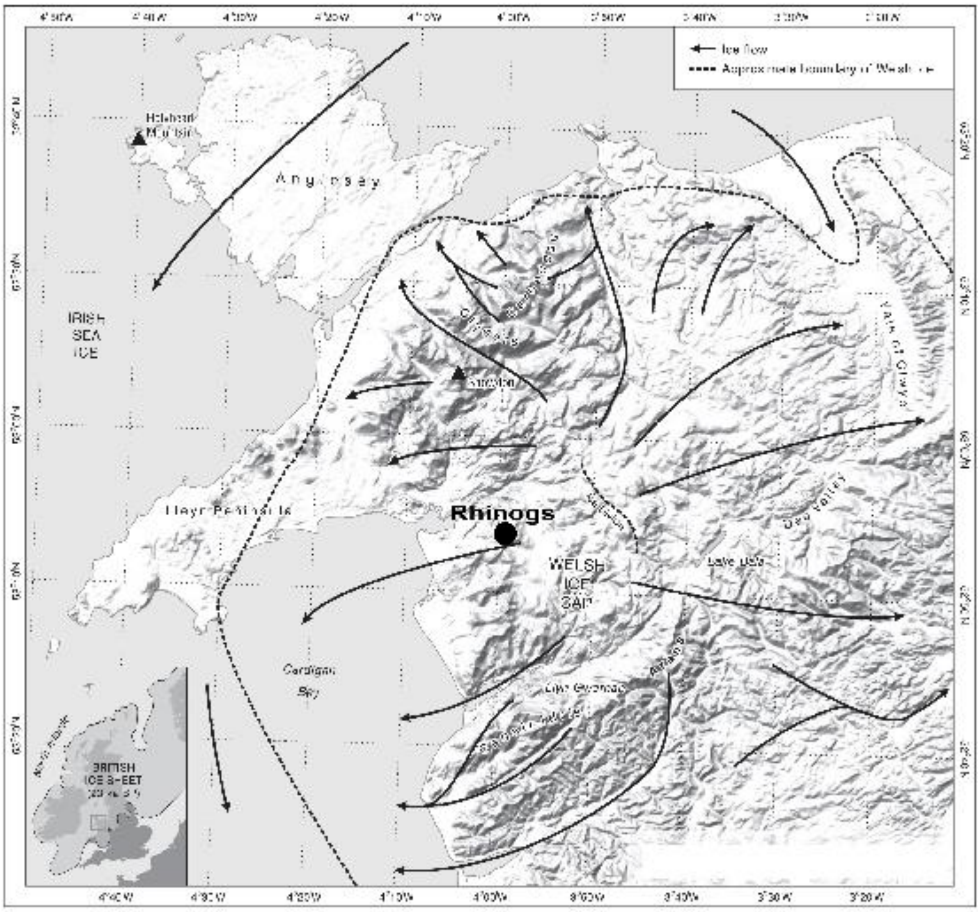

Figure 1. Overview map of North Wales including the Rhinog Mountains, showing the location of the study area with respect to the former British-Irish Ice Sheet (inset) and the Welsh Ice Cap (adapted from Hughes et al., 2016).

Figure 2 (A). Glacially eroded bedrock surface at Moel Ysgyfarnogod showing abraded bedrock pavement with striations and grooves and perched glacially transported boulders. Note the striations and grooves cross-cut the bedrock joints.

Figure 2(B). Glacially eroded bedrock surface at Moel Ysgyfarnogod showing both partially open and fully open joints with detached, quarried blocks. Former ice flow was from right to left.

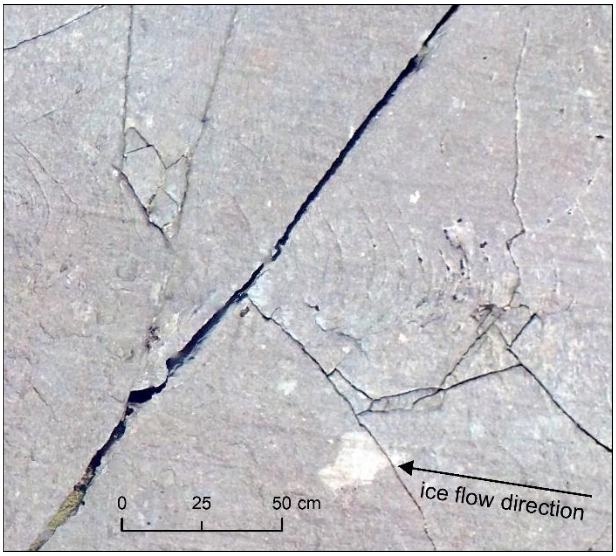

Figure 2(C). Chatter marks/crescentic fractures (centre of image) were observed on UAV photos made during a test flight on an outcrop 30 m northwest from the study site.

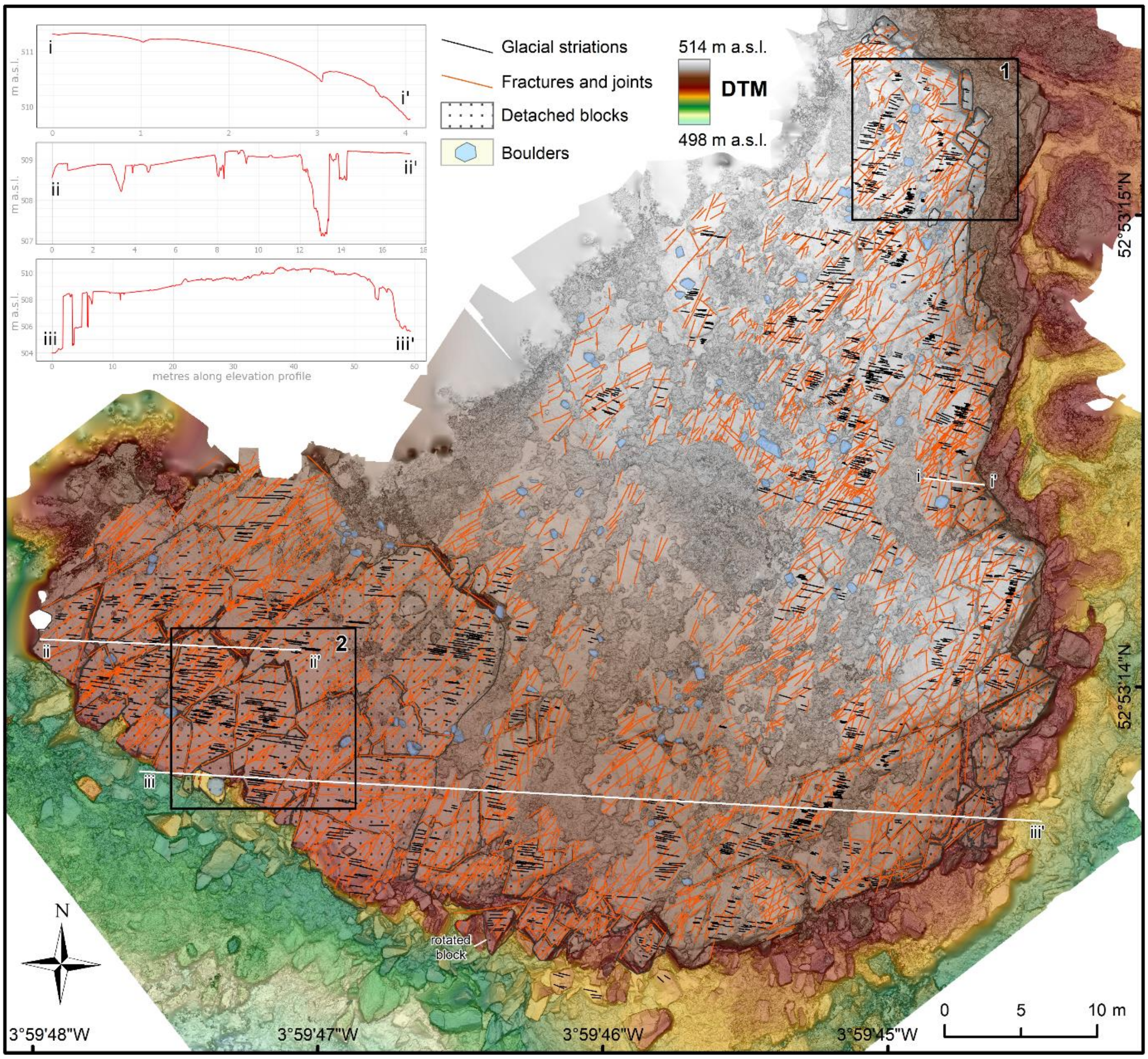

Figure 3. Digital Terrain Model of the glacially eroded bedrock surface derived from the UAV survey at Moel Ysgyfarnogod. Former ice flow direction across the bedrock surface (indicated by striations and grooves) is east to west. Note that the area dominated by large detached blocks is located on the western (distal) side of the outcrop. Three topographic profiles are shown in the upper left corner and marked by small roman ciphers in the map. Inset boxes show Area 1 and 2 described in detail in the text and shown in Figure 5. Area 1 and Profile i-i' represent the ice-moulded, abraded bedrock on the eastern, proximal side of

the outcrop, whereas Area 2 and Profile ii-ii' is the quarried bedrock on the western, lee side of the outcrop. Profile iii-iii' runs over the length of the entire outcrop. Note also the large, open fractures up to 4 m in depth on the quarried lee side of the outcrop (visible in the profiles). The volume accounted for by quarried or partially quarried bedrock blocks in this area amounts to more than 2000 m^3 (the area bounded by open joints of 50 x 10 m with a depth of at least 4 m).

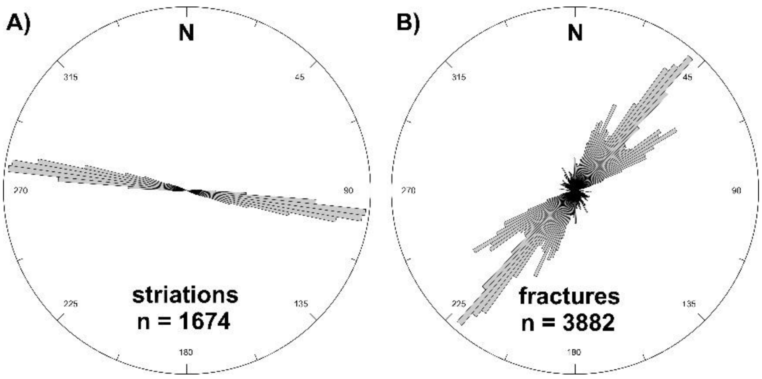

Figure 4. Stereo plots showing (A) the orientation of 1674 measured striations and grooves, and (B) the orientation of 3882 measured bedrock fracture and joint orientations at Moel Ysgyfarnogod. Note the consistent west to east alignment of the striations and grooves (median azimuth = 99–279°), which is orthogonal to the bedrock fracture and joint orientations (median azimuth = 37–217°).

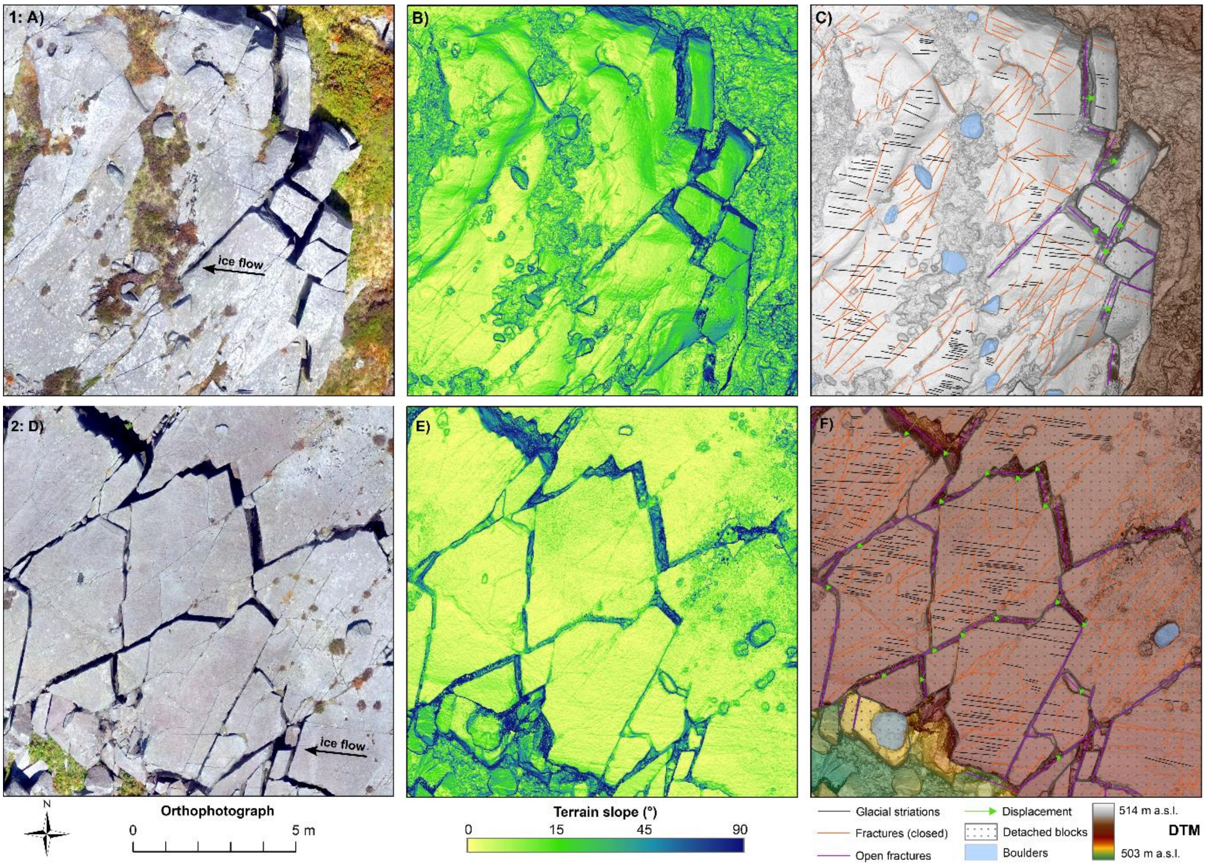

Figure 5. Detail of Area 1, the ice-moulded, abraded bedrock on the eastern side of the outcrop at Moel Ysgyfarnogod, and Area 2, the quarried bedrock on the western side. Both Areas 1 and 2 are indicated on Figure 3. Former ice-flow direction is indicated in (A) and (D). A, D) orthophoto, B, E) terrain slope, C, F) mapped bedrock features including striations and grooves, glacially transported boulders, bedrock fractures and detached blocks with inferred direction of displacement. Note the size of the detached blocks in panels D to F (dimensions of up to 5 m), which appear to have been in the process of being quarried during deglaciation. The small blocks in the upper right of panels A to C are inferred to be detached as the result of post-glacial periglacial/paraglacial processes.

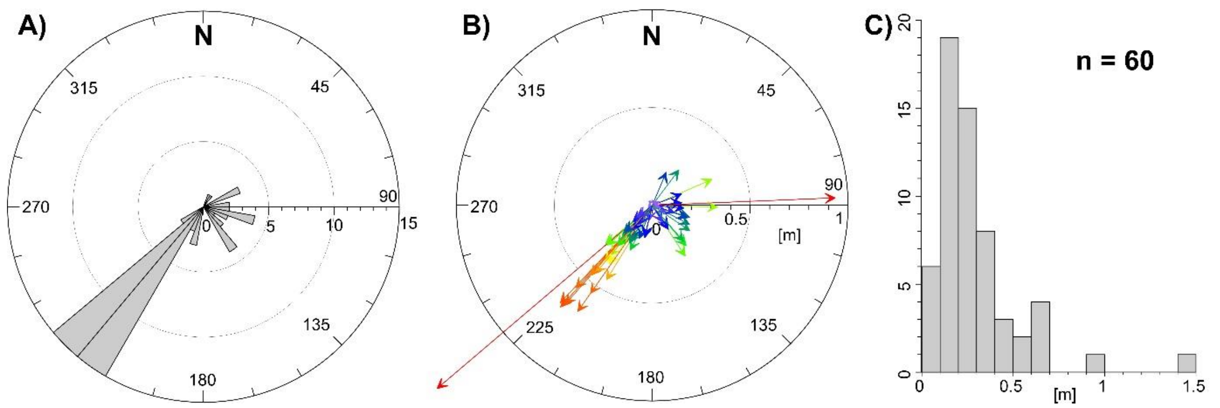

Figure 6. Quantitative information for 60 reliably measured quarried blocks at Moel Ysgyfarnogod. (A) Stereo plot histogram showing measured direction of displacement of quarried blocks. (B) Distance of displacement expressed as vectors in m. (C) Histogram

showing the frequency of distance of displacement (in m); the median and mean displacement distance was 0.21 m and 0.29 m, respectively.

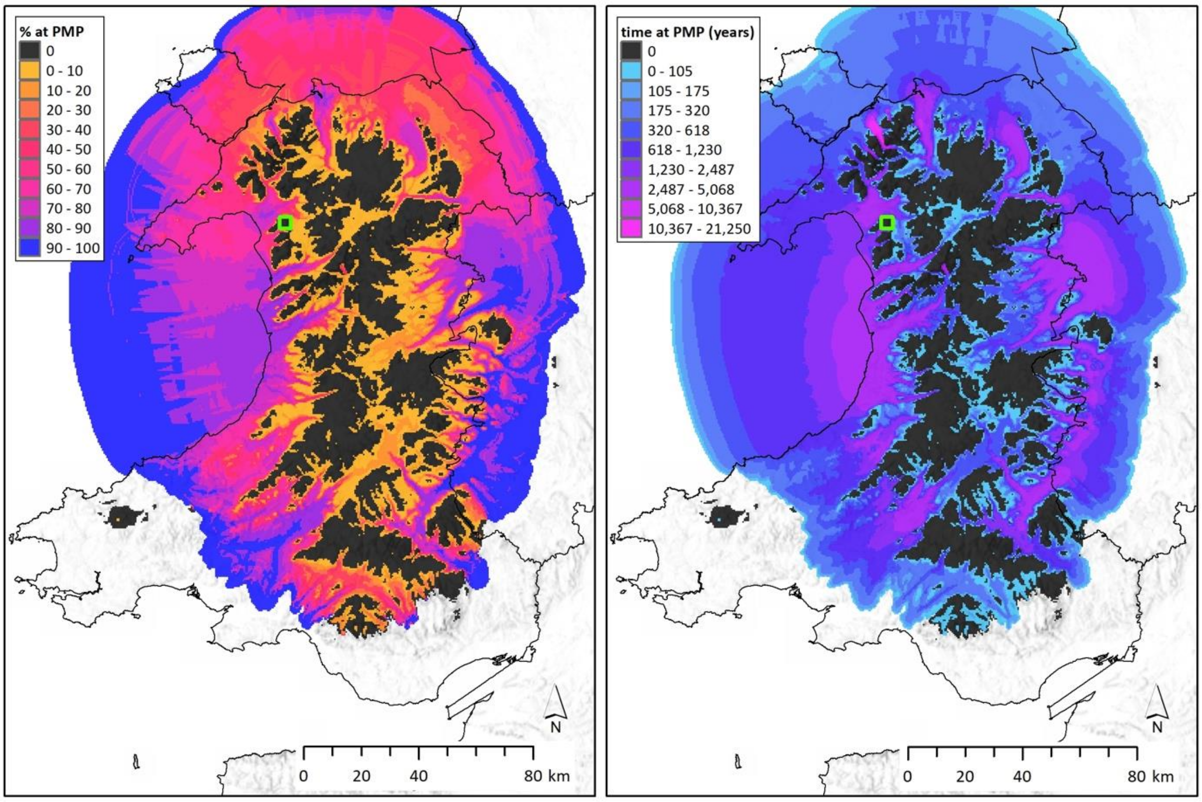

Figure 7. Results of numerical modelling of the Welsh Ice Cap showing the percentage time (left panel, in %) and total time (right panel, in years) when the basal ice was at the pressure melting point (PMP). Modified from Patton et al. (2013a, b). The position of the Rhinogs study area is indicated by the green box in North West Wales.

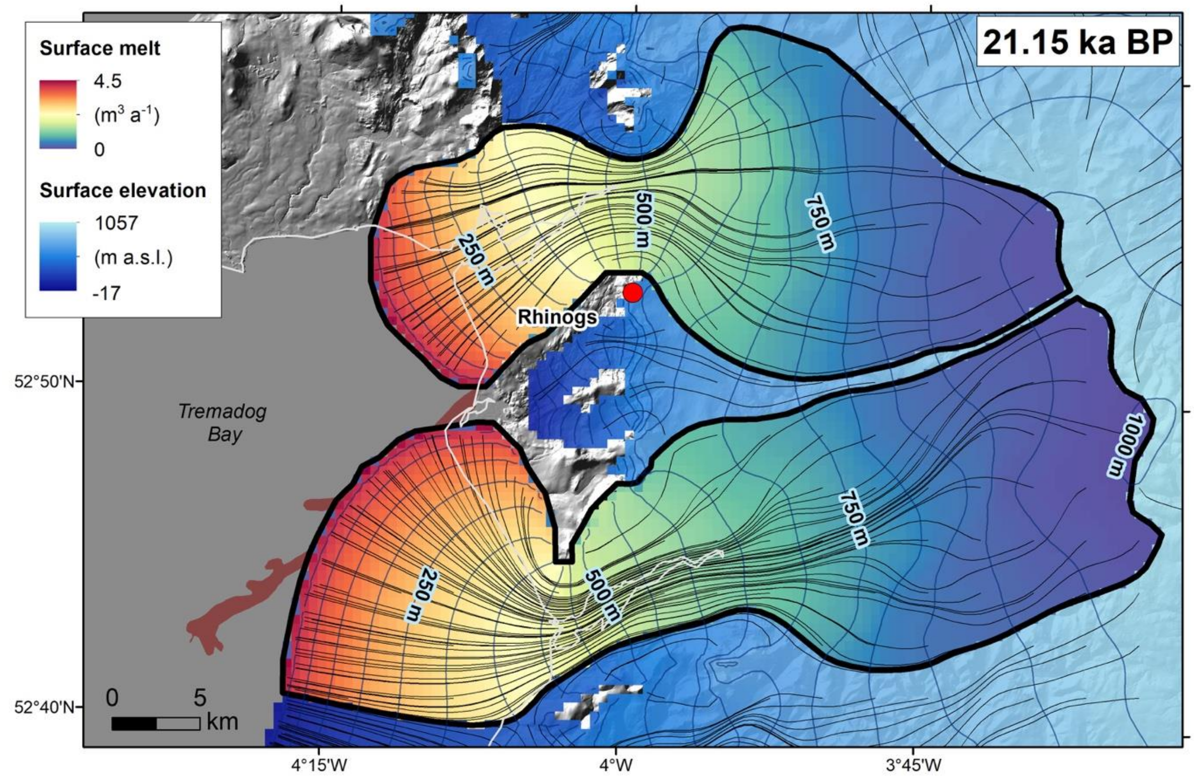

Figure 8: Results of numerical ice-sheet modelling that indicate the Welsh Ice Cap readvanced during deglaciation at 21.15 ka BP after it separated from the Irish Sea Ice Stream (Patton et al., 2013c). The major glacial catchments highlighted include the Tremadog (N) and Mawddach (S) glaciers. The position of the Rhinogs study area is indicated by the red circle.

References

Addison, K., 1997. *Classic glacial landforms of Snowdonia*. The Geographical Association, 2nd edition.

Alley, R.B., Cuffey, K.M., Zoet, L.K. 2019. Glacial erosion: status and outlook. *Annals of Glaciology*, 1–13.

Anderson, R.S., 2014. Evolution of lumpy glacial landscapes. *Geology*, 42, 679–682.

Atkins, C.B., 2013. Geomorphological evidence of cold-based glacier activity in South Victoria Land, Antarctica. In: Hambrey, M. J., Barker, P. F., Barrett, P. J., Bowman, V., Davies, B., Smellie, J. L. & Tranter, M. (eds) *Antarctic Palaeoenvironments and Earth-Surface Processes*. Geological Society, London, Special Publications, 381, 299–318.

Atkins, C.B., Barrett, P.J., Hicock, S.R., 2002. Cold glaciers erode and deposit: evidence from Allan Hills, Antarctica. *Geology,* 30, 659–662.

Ball, D.F, Goodier, R., 1968. Large sorted stone-stripes in the Rhinog Mountains, North Wales. *Geografiska Annaler: Series A: Physical Geography*, 50, 54–59.

Bartholomew, I., Nienow, P., Sole, A., Mair, D., Cowton, T., Palmer, S., Wadham, J., 2011. Supraglacial forcing of subglacial drainage in the ablation zone of the Greenland ice sheet. *Geophysical Research Letters*, 38, L08502. https://doi.org/10.1029/2011GL047063

Cohen, D., Iverson, N.R., Hooyer, T.S., Fischer, U.H., Jackson, M., Moore, P.I., 2005. Debris-bed friction of hard-bedded glaciers. *Journal of Geophysical Research*, 110, FO2007. https://doi.org/10.1029/2004JF000228

Cook, S.J., Swift, D.A., Kirkbride, M.P., Knight, P.G., Waller, R.I., 2020. The empirical basis for modelling glacial erosion rates. *Nature Communications*, 11, 1–7. https://doi.org/10.1038/s41467-020-14583-8

Cuffey, K.M., Conway, H., Gades, A.M., Hallet, B., Lorrain, R., Severinghaus, J.P., Steig, E.J., Vaughn, B., White, J.W.C., 2000. Entrainment at cold glacier beds. *Geology*, 28, 351–354.

Doyle, S.H., Hubbard, A., Van De Wal, R.S.W., Box, J.E., Van As, D., Scharrer, K., Meierbachtol, T.W., Smeets, P.C.J.P., Harper, J.T., Johansson, E., Mottram, R.H., Mikkelsen, A.B., Wilhelms, F., Patton, H., Christoffersen, P., Hubbard, B., 2015. Amplified melt and flow of the Greenland ice sheet driven by late-summer cyclonic rainfall. *Nature Geoscience*, 8, 647–653.

Dühnforth, M., Anderson, R.S., Ward, D., Stock, G.M., 2010. Bedrock fracture control of glacial erosion processes and rates. *Geology*, 38, 423–426.

EDINA Geology Digimap. 2014. British Geological Survey (BGS) data.http://edina.ac.uk/digimap/index.shtml

Evans, I.S., 1996. Abraded rock landforms (whalebacks) developed under ice streams in mountainous areas. *Annals of Glaciology*, 22, 9–16.

Fearnsides, W.G., 1905. On the geology of Arenig Fawr and Moel Llyfnant. *Quarterly Journal of the Geological Society*, 61, 608–640.

Foster, H.D., 1968. *The glaciation of the Harlech Dome*. University College London (University of London).

Foster, H.D., 1970a. Establishing the age and geomorphological significance of sorted stone-stripes in the Rhinog Mountains, North Wales. *Geografiska Annaler, Series A, Physical Geography*, 52, 96–102.

Foster, H.D., 1970b. Sarn Badrig, a submarine moraine in Cardigan Bay, north Wales. *Zeitschrift für Geomorphologie*, 14, 473–486.

Glasser, N.F., Bennett, M.R., 2004. Glacial erosional landforms: origins and significance for palaeoglaciology. *Progress in Physical Geography*, 28, 43–75.

Glasser, N.F., Crawford, K.R., Hambrey, M.J., Bennett, M.R., Huddart, D., 1998. Lithological and structural controls on the surface wear characteristics of glaciated metamorphic bedrock surfaces: Ossian Sarsfjellet, Svalbard. *The Journal of Geology*, 106, 319–330.

Glasser, N. F., Hughes, P. D., Fenton, C., Schnabel, C., Rother, H., 2012. ^{10}Be and ^{26}Al exposure-age dating of bedrock surfaces on the Aran ridge, Wales: evidence for a thick Welsh Ice Cap at the Last Glacial Maximum. *Journal of Quaternary Science*, 27, 97–104.

Gordon, J.E., 1981. Ice-scoured topography and its relationship to bedrock structure and ice movements in parts of northern Scotland and west Greenland. *Geografiska Annaler, Series A, Physical Geography*, 63, 55–65.

Greenly, E., 1919. *The Geology of Anglesey*. Memoirs of the Geological Survey of Great Britain, HMSO, London.

Groos, A.R., Bertschinger, T.J., Kummer, C.M., Erlwein, S., Munz, L., Philipp, A., 2019. The potential of low-cost UAVs and open-source photogrammetry software for high-resolution monitoring of alpine glaciers: A case study from the Kanderfirn (Swiss Alps). Geosciences, 9(356). doi:10.3390/geosciences9080356

Hallet, B., 1979. A theoretical model of glacial abrasion. *Journal of Glaciology*, 23, 39–50.

Hallet, B., 1996. Glacial quarrying: a simple theoretical model. *Annals of Glaciology*, 22, 1–8.

Herman, F., Beyssac, O., Brughelli, M., Lane, S.N., Leprince, S., Adatte, T., Lin, J.Y., Avouac, J.P., Cox, S.C., 2015. Erosion by an Alpine glacier. *Science*, 350, 193–195.

Hooyer, T.S., Cohen, D., Iverson, N.R., 2012. Control of glacial quarrying by bedrock joints. *Geomorphology*, 153, 91–101.

Hughes, P.D., Glasser, N.F., Fink, D., 2016. Rapid thinning of the Welsh Ice Cap at 20 ka based on ^{10}Be ages. *Quaternary Research*, 85, 107–117.

Iverson, N., 1991. Potential effects of subglacial water-pressure fluctuations on quarrying. *Journal of Glaciology*, 328, 27–36.

Iverson, N., 2012. A theory of glacial quarrying for landscape evolution models. *Geology*, 40, 679–330.

Jahns, R.H., 1943. Sheet structure in granites; its origin and use as a measure of glacial erosion in New England. *Journal of Geology*, 51, 71–98.

Jansson, K.N., Glasser, N.F., 2005. Palaeoglaciology of the Welsh sector of the British–Irish Ice Sheet. *Journal of the Geological Society*, London, 162, 25–37.

Jones, C., Ryan, J., Holt, T., Hubbard, A., 2018. Structural glaciology of Isunguata Sermia, West Greenland. *Journal of Maps*, 14, 517–527.

Krabbendam, M., Bradwell, T., Everest, J.D., Eyles, N., 2017. Joint-bounded crescentic scars formed by subglacial clast-bed contact forces: Implications for bedrock failure beneath glaciers. *Geomorphology*, 290, 114–127.

Krabbendam, M., Glasser, N.F., 2011. Glacial erosion and bedrock properties in NW Scotland: abrasion and plucking, hardness and joint spacing. *Geomorphology*, 130, 374–383.

Lane, T.P., Roberts, D.H., Rea, B.R., Ó Cofaigh, C., Vieli, A., 2015. Controls on bedrock bedform development beneath the Uummannaq Ice Stream onset zone, West Greenland. *Geomorphology*, 231, 301–313.

Lee, J.R., Rose, J., Hamblin, R.J.O., Moorlock, B.S.P., Riding, J.B., Phillips, E., Barendregt, R.W., Candy, I., 2011. The Glacial History of the British Isles during the Early and Middle Pleistocene: Implications for the long-term development of the British Ice Sheet. In: Ehlers, J., Gibbard, P.L. & Hughes, P.D (eds) *Quaternary glaciations – extent and chronology*. Elsevier, Amsterdam, 59–74.

Patton, H., Hubbard, A., Glasser, N.F., Bradwell, T., Golledge, N.R., 2013a. The last Welsh Ice Cap: Part 1 – Modelling its evolution, sensitivity and associated climate. *Boreas*, 42, 471–490.

Patton, H., Hubbard, A., Glasser, N.F., Bradwell, T., Golledge, N.R., 2013b. The last Welsh Ice Cap: Part 2 – Dynamics of a topographically controlled ice cap. *Boreas*, 42, 491–510.

Patton, H., Hubbard, A.L., Bradwell, T., Glasser, N.F., Hambrey, M.J., Clark, C.D., 2013c. Rapid marine deglaciation: asynchronous retreat dynamics between the Irish Sea Ice Stream and terrestrial outlet glaciers. *Earth Surface Dynamics*, 1, 53–65.

Piermattei, L., Carturan, L., De Blasi, F., Tarolli, P., Dalla Fontana, G., Vettore, A., Pfeifer, N., 2016. Suitability of ground-based SfM-MVS for monitoring glacial and periglacial processes. *Earth Surface Dynamics*, 4, 425–443.

Roberts, D.H., Long, A.L., 2005. Streamlined bedrock terrain and fast ice flow, Jakobshavn Isbrae, West Greenland: implications for ice stream and ice sheet dynamics. *Boreas*, 34, 25–42.

Ryan, J.C., Hubbard, A.L., Box, J.E., Todd, J., Christoffersen, P., Carr, J.R., Holt, T.O., Snooke, N.A., 2015. UAV photogrammetry and structure from motion to assess calving dynamics at Store Glacier, a large outlet draining the Greenland ice sheet. *The Cryosphere*, 9, 1–11.

Sharp, M., Dowdeswell, J.A., Gemmell, J.C., 1989. Reconstructing past glacier dynamics and erosion from glacial geomorphic evidence; Snowdon, North Wales. *Journal of Quaternary Science*, 4, 115–130.

Sugden, D.E., John, B.S., 1976. *Glaciers and landscape: a geomorphological approach*. Edward Arnold.

Sugden, D.E., Glasser, N.F., Clapperton, C.M., 1992. Evolution of large roches moutonnées. *Geografiska Annaler, Series A: Physical Geography*, 74, 253–264.

Sugden, D.E., Hall, A.M., Phillips, W.M., Stewart, M.A. 2019. Plucking enhanced beneath ice sheet margins: evidence from the Grampian Mountains, Scotland. *Geografiska Annaler, Series A: Physical Geography*, 101, 34–44.

Ugelvig, S.V., Egholm, D.L., Anderson, R.S., Iverson, N.R., 2018. Glacial erosion driven by variations in meltwater drainage. *Journal of Geophysical Research: Earth Surface*, 123, 2863–2877.

Verma, A.K., Bourke, M.C., 2019. A method based on structure-from-motion photogrammetry to generate sub-millimetre-resolution digital elevation models for investigating rock breakdown features. *Earth Surface Dynamics*, 7, 45–66.

Westoby, M.J., Brasington, J., Glasser, N.F., Hambrey, M.J., Reynolds, J.M., 2012. 'Structure-from-Motion' photogrammetry: A low-cost, effective tool for geoscience applications. *Geomorphology*, 179, 300–314.

Yanites, B.J., Ehlers, T.A., 2016. Intermittent glacial sliding velocities explain variations in long-timescale denudation. *Earth and Planetary Science Letters*, 450, 52–61.

Zoet, L.K, Alley, R.B., Anandakrishnan, S., Christianson, K. 2013. Accelerated subglacial erosion in response to stick-slip motion. *Geology*, 41, 159–162.

683